Journal of the European Ceramic Society 21 (2001) 2835–2841
www.elsevier.com/locate/jeurceramsoc

Crystallization behaviour of glasses produced from fly ash

M. Erol [a,*], S. Küçükbayrak [a], A. Ersoy-Meriçboyu [a], M.L. Öveçoğlu [b]

[a] *Department of Chemical Engineering, Chemical and Metallurgical Engineering Faculty, Istanbul Technical University, Maslak 80626, Istanbul, Turkey*
[b] *Department of Metallurgical and Materials Engineering, Chemical and Metallurgical Engineering Faculty, Istanbul Technical University, Maslak 80626, Istanbul, Turkey*

Received 12 October 2000; received in revised form 10 January 2001; accepted 20 January 2001

Abstract

The crystallization behaviour of fly ash based glass samples annealed at 600°C for 2 and 10 h was investigated by DTA, XRD and SEM. On the basis of DTA, nucleation experiments of two glass samples were carried out at 680 and 687°C for 5 h and crystallization experiments were performed at 924 and 892°C for 20 min. The Avrami constant for both glass samples was calculated as 4, which indicates bulk crystallization, predicted by the Ozawa equation. Using the modified Kissinger equation, activation energies of crystal growth were determined as 318 and 312 kJ/mol for samples annealed at 2 and 10 h, respectively. Single peak analysis technique proved that the activation energy is independent of DTA heating rate. SEM observations indicated that the produced glass–ceramic samples have fine grained microstructure. The crystallized phase was identified as diopside [$Ca(Mg,Al)(Si,Al)_2O_6$] by X-ray diffraction analysis. The results of Vickers microhardness tests showed that the hardness values of the produced glass–ceramic samples decreased with the increase in holding time at the annealing temperature.

Keywords: Crystallization kinetics; Fly ash; Glasses; Glass–ceramics; Hardness; Waste materials

1. Introduction

Fly ash is a waste material produced from coal burning thermal power plants. Since it is in dry form and produced in large quantities, it is one of the major source for environmental pollution. In recent years, many research and development investigations have been conducted in its utilization as a starting material for glass–ceramic production.[1–5] Furthermore, fly ash is much more convenient than steel slags in glass ceramic production: it is available in fine powder form and in greater quantities than slag.

Glass–ceramics are polycrystalline solids produced by controlled crystallization of glasses.[6] Controlled crystallization usually involves a two-stage heat treatment, namely a nucleation stage and a crystallization stage. In the nucleation stage, small nuclei are formed within the parent glass. After the formation of stable nuclei, crystallization proceeds by growth of a new crystalline phase. Knowledge of nucleation and crystallization parameters is important in the preparation of glass–ceramics with desired microstructure and properties.[7]

Differential thermal analysis (DTA) is widely used in investigating the crystallization kinetics of glasses and glass-ceramics.[1,8–20] Two methods, namely isothermal and non-isothermal methods, are applied for differential thermal analysis. In the isothermal method, glass samples are quickly heated up and held at a temperature above the glass transition temperature. In this case crystallization occurs at a constant temperature. In the non-isothermal method, glass samples are heated up at a fixed heating rate and crystallized during the thermal analysis scan.[9] The non-isothermal method is more simple and quicker than the isothermal method. Activation energy and crystallization mechanisms are the most important kinetic parameters for the crystallization of glasses. These parameters can be obtained by DTA results using the equations that are proposed to interpret non-isothermal data.[19–24]

The aim of the present work is to investigate the effect of different holding times during annealing temperature on the crystallization behaviour of fly ash based glasses

* Corresponding author. Tel.: +90-212-285-3351; fax: +90-212-285-2925.
E-mail address: erolm@itu.edu.tr (M. Erol).

0955-2219/01/$ - see front matter
PII: S0955-2219(01)00221-7

and to determine some kinetic parameters that describe the crystallization process by DTA.

2. Experimental procedure

2.1. Thermal analysis and heat treatment

The detailed procedure of the glass production from fly ash which consists of chemically following oxides (in wt.%); 42.82% SiO_2, 16.38% CaO, 5.85% MgO, 7.01% Fe_2O_3, 13.36% Al_2O_3, 5.06% Na_2O, 1.83% K_2O and 6.47% SO_3 has been described previously.[25] The as-cast glass samples were annealed at 600°C for 2 and 10 h followed by slow cooling to the room temperature.

Differential thermal analysis (DTA) scans of annealed glass specimens were carried out in a Rigaku Thermoflex Thermal Analyzer. After crushing annealed glasses to the size of about 1 mm, non-isothermal experiments were performed by heating 30 mg glass samples in a Pt-crucible and using Al_2O_3 as the reference material in the temperature range between 20 and 1100°C at the heating rates of 5, 10, 15 and 20°C/min. Kissinger[15,19,26] and Ozawa[21] analyses were applied to the DTA scan results to obtain the activation energy for crystallization and the crystallization mechanism of the glass–ceramic samples, respectively. Activation energy is also determined by using a single crystallization peak analysis technique.

Nucleation and crystallization experiments were carried out on the basis of DTA scan results. The peak temperatures (T_g and T_p) changing with heating rates were given in Table 1. Nucleation and crystallization temperatures were selected 10°C above the T_g and T_p temperatures. Preliminary qualitative optical microscopy work was carried out on as-cast glass specimens (2 h at 600°C and 10 h at 600°C) heated slightly above the T_g value for different temperatures and held at these temperatures 5 h followed by quenching in water to observe the development of the stable nuclei.[27,28] Optical samples revealed the highest amount of visible nuclei which did not increase in number at longer times and the stable nuclei formed in the microstructure only 10°C above the glass transition temperatures.[25] On the basis of this observation, the optimum nucleation temperatures chosen for this study were 680 and 687°C. The annealing temperature was chosen as 600°C. As reported in the literature, 70–100°C below the T_g value is appropriate for the annealing temperature.[2,29] For this purpose, glass samples annealed at 600°C for 2 and 10 h were heated at a rate of 10°C/min to the nucleation temperature of 680 and 687°C, respectively. In the previous study regarding the crystallization behaviour of fly ash,[25] an optimum nucleation time of 5 h was determined at these nucleation temperatures. Following nucleation, the temperature was raised to the crystallization temperatures of 924 and 892°C, for the samples annealed for 2 and 10 h, respectively. Samples were held at these temperatures for 20 min and cooled in the furnace.

Table 1
T_g and T_p values of glasses produced from fly ash

Heating rate (°C/min)	Peak temperatures (°C)			
	T_g		T_p	
	2 h at 600°C	10 h at 600°C	2 h at 600°C	10 h at 600°C
5	663	674	883	863
10	671	677	914	882
15	682	684	935	917
20	685	692	950	919

2.2. Microstructural characterizations and mechanical tests

The characterization of the produced glass–ceramic samples was carried out using both electron microscopy and X-ray diffraction techniques. Scanning electron microscopy (SEM) investigations were conducted in a Jeol™ Model JSM-T330 operated at 25 kV and linked with an energy dispersive (EDS) attachment. For the SEM investigations, optical mount specimens were prepared using standard metallographic techniques followed by chemical etching them in a HF solution (5%) for 1.5 min. The etched glass–ceramic samples were coated with a thin layer of gold.

The X-ray diffraction (XRD) investigations were carried out in a Philips™ Model PW3710 using CuK_α radiation at 40 kV and 40 mV settings in the 2θ range from 10 to 80°. The crystallized phases were identified by comparing the peak positions and intensities with those in the JCPDS (Joint Committee on Powder Diffraction Standards) data files.

Vickers microhardness measurements of heat treated glass–ceramic samples were made with a LL Model Tukon Tester. Specimens were prepared using conventional metallographic techniques and a load of 500 g were used to indent their surfaces. In order to obtain reliable statistical data, at least 15 indentations were made on each sample.

3. Results and discussions

3.1. Activation energy determination

DTA experiments were carried out on annealed glass samples to investigate the crystallization behaviour of the glasses. Figs. 1 and 2 show the DTA scan curves of glasses annealed at 600°C for 2 and 10 h. As seen in Figs. 1 and 2, the faster the heating rates, the higher the peak temperatures and the larger the peak heights

become. The crystallization peak temperature, T_p, decreases with increase in the holding time at the annealing temperature. A broad crystallization peak indicates surface crystallization, whereas a sharp peak signifies a bulk crystallization process.[21] Based on this interpretation, it can be inferred that bulk crystallization is predominant in the produced glass samples.

The variation of the crystallization peaks with different DTA heating rates can be used to estimate the activation energy for crystallization and to determine the crystallization mechanism. The activation energy for the crystallization of the glass samples can be determined by using the modified Kissinger method as described by Matusiata et al.[15,19,26] The crystallization peak temperature is obtained as a function of the heating rate, then the following relationship is applied:

$$\ln\left(\phi^n/T_p^2\right) = -\left(mE/RT_p\right) + \text{constant} \quad (1)$$

Where ϕ is the heating rate, T_p is the crystallization peak temperature at a given heating rate, E is the activation energy for crystallization, R is the gas constant, n is an Avrami constant and m is the dimensionality of crystal growth. The parameters n and m are characteristics of various crystallization mechanisms and they can take on various values as summarized in Table 2.[15,19,30] For the special case where surface crystallization is the predominant mechanism, $n=m=1$, Eq. (1) reduces to the familiar Kissinger equation.[31]

The value of the Avrami constant, n, can be determined by the Ozawa equation:[21]

$$\left|\frac{\mathrm{d}(\ln - \ln(1-x))}{\mathrm{d}\ln\phi}\right|_T = -n \quad (2)$$

where x is the volume fraction crystallized at a fixed temperature T with the heating rate of ϕ. x is the ratio of the partial area at a certain temperature to the total area of a crystallization exotherm. Plots of $\ln(-(\ln(1-x)))_T$ vs $\ln\phi$ for glass samples annealed at 600°C for 2 and 10 h are shown in Figs. 3 and 4, and the values of n determined from the slopes of these plots are 4 and 3.8 (allowing experimental errors, the latter value is close to 4), respectively. These values indicate that the bulk crystallization is dominant in the produced glass. The m value for the glass samples annealed at 600°C for 2 and 10 h should be equal to $n-1$, i.e. 3. By substituting the appropriate values of n, m and R (8.3144 J/mol K) in Eq. (1) for two glass samples, the activation energies are found from the slope ($-mE/R$) of a plot of $\ln\left(\phi^n/T_p^2\right)$

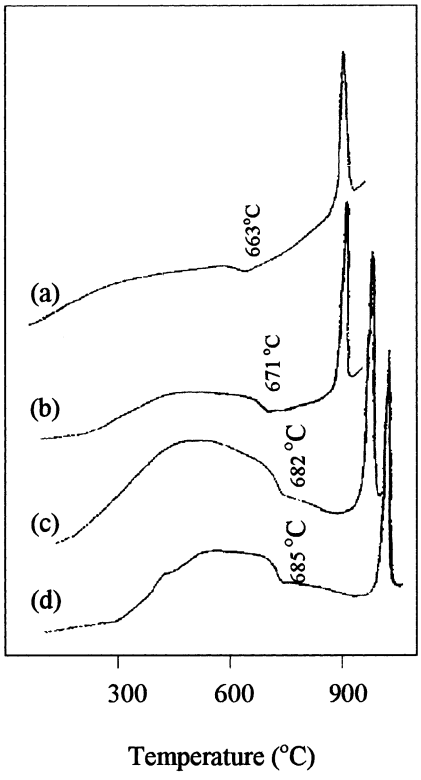

Fig. 1. DTA plots of the as-cast glass annealed at 600°C for 2 h scanned at the heating rates of: (a) 5°C/min, (b) 10°C/min, (c) 15°C/min and (d) 20°C/min.

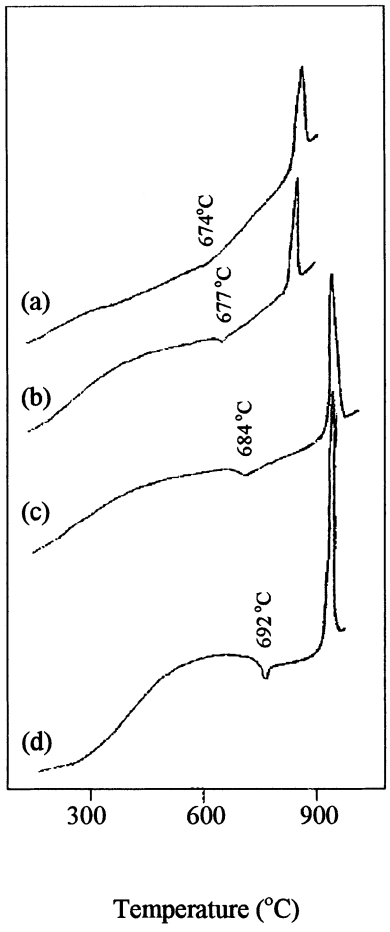

Fig. 2. DTA plots of the as-cast glass annealed at 600°C for 10 h scanned at the heating rates of: (a) 5°C/min, (b) 10°C/min, (c) 15°C/min and (d) 20°C/min.

against $1/T_p$. The modified Kissinger plots were presented in Figs. 5 and 6. From the slope of the modified Kissinger plots, the activation energies for the crystallized glass samples annealed at 600°C for 2 and 10 h were determined as 318 and 312 kJ/mol, respectively. Since both samples have the same composition, calculated activation energy values, E, are very close to each other. The calculated activation energy values are lower than the value of 370 kJ/mol found by Cioffi et al.[1] for a glass–ceramic produced from fly ash.

Activation energy for any of the glass sample can also be determined from a single DTA peak using the following equation:[15]

$$\ln(-\ln(1-x)) = -mE/RT + \text{constant} \quad (3)$$

x is the volume fraction crystallized at different temperatures (T) for a single crystallization exotherm. E can be calculated from the slope of ln $(-\ln(1-x))$ vs $1/T$. Eq. (3) is also used to determine the effect of heating rate (ϕ) on activation energy (E). The plots of $\ln(-\ln(1-x))$ vs $1/T$ for the crystallization peak determined at heating rates of 5, 10, 15 and 20°C/min are shown in Figs. 7 and 8 for samples annealed at 600°C for 2 and 10 h, respectively. Table 3 represents the activation energy values that are determined individually from the crystallization peaks. As seen in Table 3, activation energy values for both samples are independent of heating rates (within the ±20 kJ/mol error). The average activation energy values for all heating rates are very close

Table 2
Values of n and m for different crystallization mechanisms in the heating process[15,19,30]

Crystallization mechanism	n	m
Bulk crystallization with a constant number of nuclei (i.e. the number of nuclei is independent of the heating rate)		
Three-dimensional growth of crystals	3	3
Two-dimensional growth of crystals	2	2
One-dimensional growth of crystals	1	1
Bulk crystallization with an increasing number of nuclei (i.e. the number of nuclei is inversely proportional to the heating rate)		
Three-dimensional growth of crystals	4	3
Two-dimensional growth of crystals	3	2
One-dimensional growth of crystals	2	1
Surface crystallization	1	1

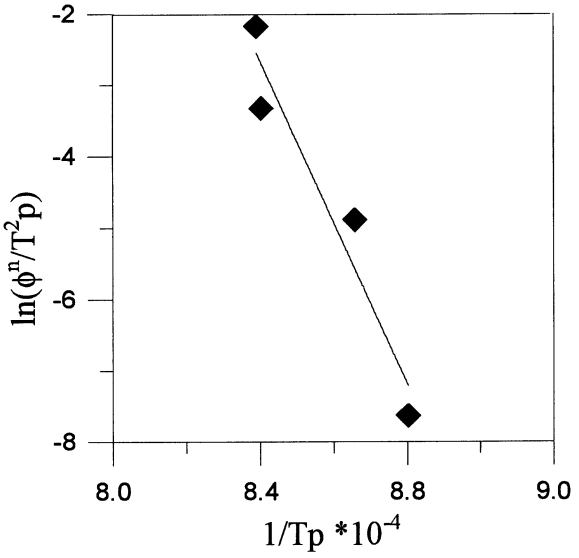

Fig. 3. The Ozawa plot of the glass sample annealed at 600°C for 2 h.

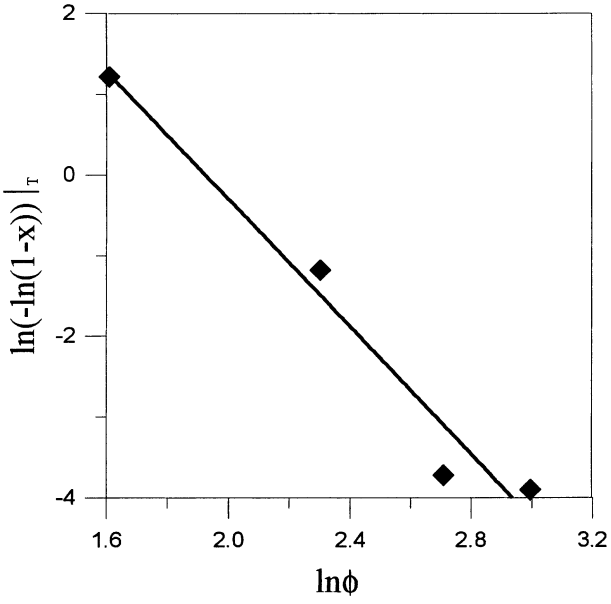

Fig. 4. The Ozawa plot of the glass sample annealed at 600°C for 10 h.

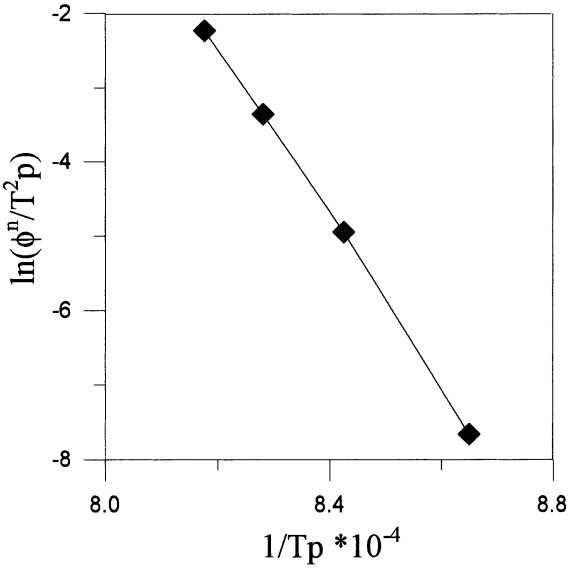

Fig. 5. The modified Kissinger plot of the glass sample annealed at 600°C for 2 h (Avrami parameter: $n=4$ and dimensionality of crystal growth: $m=3$).

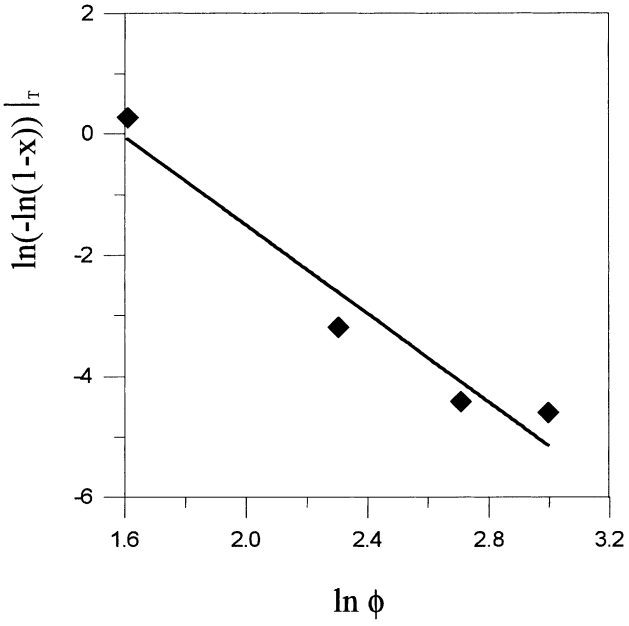

Fig. 6. The modified Kissinger plot of the glass sample annealed at 600°C for 10 h (Avrami parameter: $n=4$ and dimensionality of crystal growth: $m=3$).

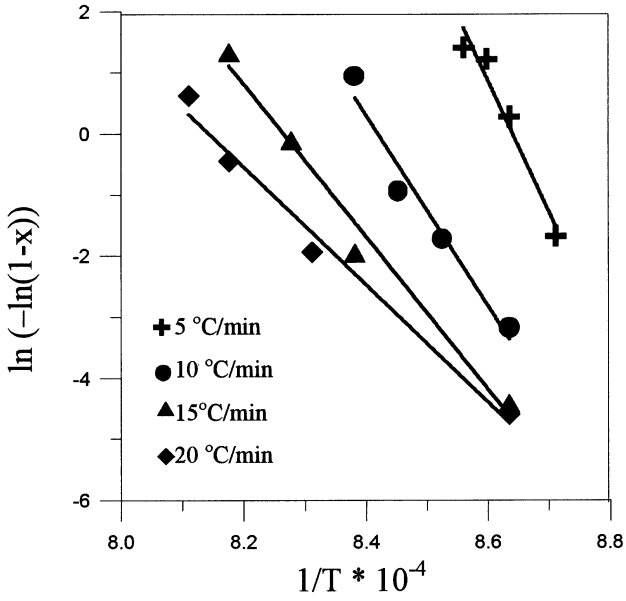

Fig. 8. Plots of $\ln(-\ln(1-x))$ vs $1/T\times10^{-4}$ for the glass sample annealed at 600°C for 10 h.

to values which are calculated from the modified Kissinger equation. However, the single peak analysis technique is very useful to determine the activation energy when only a small amount of glass is available or the quick determination of activation energy using with only one DTA measurement is required and the m value is known.

3.2. Microstructral characterization

To determine the morphology of the microstructure, SEM investigations were applied on the produced glass–ceramic samples. Fig. 9 shows the SEM micrograph of the glass–ceramic sample nucleated at 680°C for 5 h and crystallized at 924°C for 20 min. A great number of crystallites approximately 0.25 μm in diameter can be seen in this figure. The crystallized glass consists of tiny spherulite crystals uniformly dispersed in the microstructure. Fig. 10 is a SEM micrograph of the glass–ceramic sample nucleated at 687°C for 5 h and crystallized at 892°C for 20 min. Fig. 10 shows the presence of a homogeneous dispersion of tiny crystallites and the average crystalline size is about 0.5 μm. The crystallites are larger than that of the glass–ceramic sample nucleated at 680°C for 5 h because of increase in the holding time at the annealing temperature. The shape of the crystallites is also changed. The sample annealed at 600°C for 2 h has more spherulitic crystallites than the sample annealed at 600°C for 10 h. Since presence of a homogenously dispersed tiny crystals in the microstructure is required, 10 h is an excessively long holding time for annealing. Cross-sectional SEM investigations were also carried out to characterize the crystallite morphology in the bulk of the samples. It was found that the similar average crystalline size and morphologies were

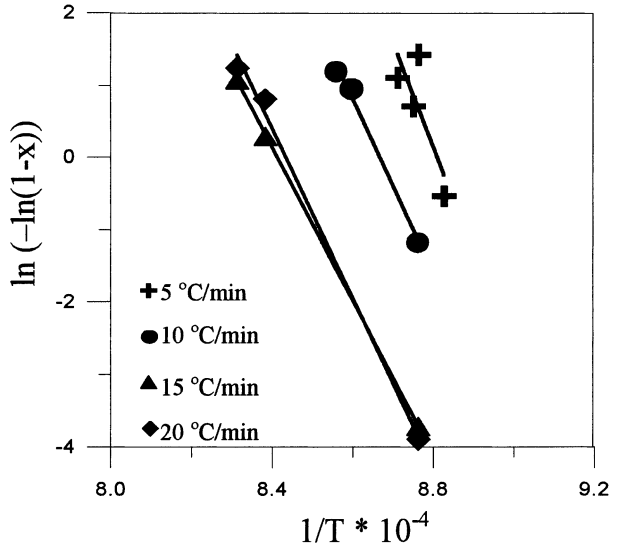

Fig. 7. Plots of $\ln(-\ln(1-x))$ vs $1/T\times10^{-4}$ for the glass sample annealed at 600°C for 2 h.

Table 3
The values of activation energy determined by using single peak analysis technique for crystallization of glass samples annealed at 2 and 10 h

	Activation energy (kJ/mol)				
Glass sample	5°C/min	10°C/min	15°C/min	20°C/min	Average
Annealed 2 h	351	355	300	330	329
Annealed 10 h	350	355	275	300	320

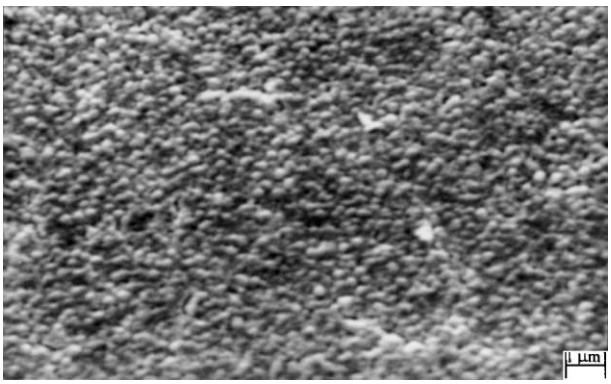

Fig. 9. Representative SEM micrograph of the fly ash based glass–ceramic sample annealed for 2 h nucleated at 680°C for 5 h and crystallized at 924°C for 20 min (magnification ×7500).

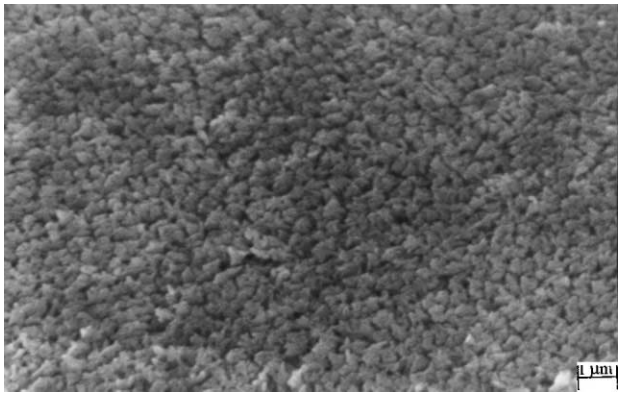

Fig. 10. Representative SEM micrograph of the fly ash based glass–ceramic sample annealed for 10 h nucleated at 687°C for 5 h and crystallized at 892°C for 20 min (magnification ×7500).

also detected in the cross-sectional SEM investigations. This confirms that bulk crystallization is the predominant mechanism in both samples as predicted by the activation energy determination in the previous section.

The crystalline phase was identified by XRD analysis. The XRD scans revealed that the main crystalline phase is diopside-alumina [Ca(Mg, Al)(Si, $Al)_2O_6$] for both glass–ceramic samples, since the glass–ceramic samples have the same composition. Fig. 11 shows the XRD pattern of the glass–ceramic sample nucleated at 680°C for 5 h.

As seen in Fig. 11, all the diffraction peaks can be indexed as arising from the reflection planes of the diopside-alumina phase which has a monoclinic structure with lattice parameters $a=0.973$ nm, $b=0.887$ nm, $c=0.528$ nm and $\beta=105.92°$.[32]

3.3. Hardness measurements

Vickers microhardness measurements taken from the glass–ceramics annealed at 600°C for 2 and 10 h yielded the values of 907 and 729 kg/mm^2, respectively. It is clear that hardness values decrease with the increase in the holding time at the annealing temperature. This is expected since the average crystalline size increases with the increase in holding time at the annealing temperature as seen in SEM micrographs (Figs. 9 and 10). In compliance with the Hall–Petch relation, the microhardness values are larger for the glass-ceramic with smaller grain size(annealed at 600°C for 2 h). The smaller the crystalline grain size the better the microhardness value.

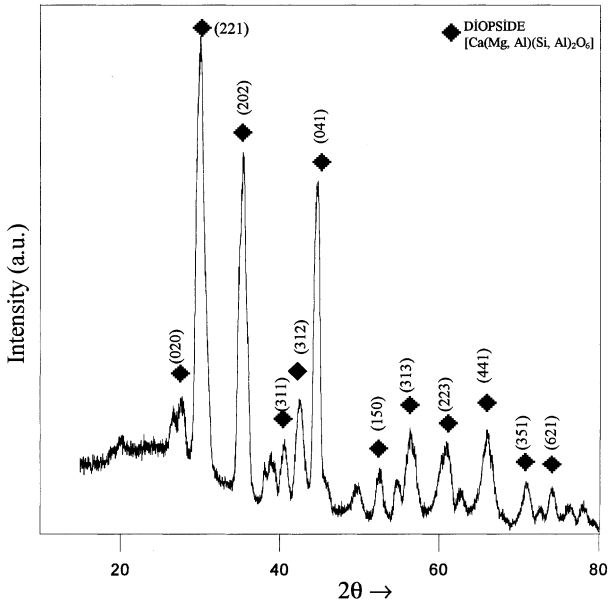

Fig. 11. X-ray diffraction pattern of the fly ash based glass–ceramic annealed for 10 h nucleated at 687°C for 5 h and crystallized at 892°C for 20 min.

4. Conclusions

From the experimental results the following conclusions can be drawn.

1. DTA results showed that the crystallization temperature varied from 863 to 950°C with the increase in the heating rate.
2. The crystallization behaviour of glass–ceramic samples has been investigated under non-isothermal conditions. Using the Ozawa equation, the Avrami constant (n) was calculated as 4 for both samples, indicating that bulk nucleation occurs in both glasses by three dimensional growth. The activation energy of crystal growth for the glass-ceramic samples annealed at 600°C for 2 and 10 h were determined using the modified Kissinger equation. The values are 318 and 312 kJ/mol, respectively. It has been shown that the activation energy is independent of the DTA heating rate.
3. XRD results revealed that the glass–ceramic samples with different heating conditions have the

same crystalline phase determined as the diopside-alumina [$Ca(Mg, Al)(Si, Al)_2O_6$] phase.

4. SEM investigations revealed that tiny crystallites ranging in size between 0.25 and 0.5 μm were uniformly dispersed in the microstructure for both samples. Similar crystalline morphology and sizes were also observed in the cross-sectional microstructures as a result of bulk crystallization in both samples.
5. The microhardness values of the produced glass–ceramics decrease with increase in the holding time at the annealing temperature.

References

1. Cioffi, R., Pernice, P., Aronne, A. and Quattroni, G., Nucleation and crystal growth in fly ash derived glass. *J. Mater. Sci.*, 1993, **28**, 6591–6594.
2. Barbieri, L., Manfredini, T., Quralt, I., Rincan, J. M. and Romero, M., Vitrification of fly ash from thermal power stations. *Glass Technology*, 1997, **38**(5), 165–170.
3. Dinu, M., Crystallization kinetics of some fly ash glasses. *Materiale de Constructi*, 1998, **28**(2), 131–134.
4. De Guive, E. J. and Risbud, S. H., Crystallization and properties of glasses prepared from illinois coal fly ash. *J. Mater. Sci.*, 1994, **19**, 1760–1766.
5. Barbieri, L., Lancelotti, I., Manfredini, T., Queralt, I., Rincan, J. M. and Romero, M., Design, obtainment and properties of glasses and glass–ceramics from coal fly ash. *Fuel*, 1999, **78**, 271–276.
6. McMillan, P. W., *Glass-ceramics*, end edn. Academic Press, London, New York, San Fransisco, 1979.
7. Strnad, Z., *Glass-ceramic Materials*. Elsevier Science, Amsterdam, 1986.
8. Sung, Y. M. and Sung, J. H., Crystallization behaviour of calcium aluminate glass fibres. *J. Mater. Sci.*, 1998, **33**, 4733–4737.
9. Cheng, K., Determining crystallization kinetic parameters of LiO_2–Al_2O_3–SiO_2 glass from derivative differential thermal analysis curves. *Mat. Sci. Eng. B*, 1999, **60**, 194–199.
10. Alizadeh, P. and Marghussian, V. K., The effect of compositional changes on the crystallization behavior and mechanical properties of diopside wollostanite glass-ceramics in the SiO_2–CaO–MgO–(Na_2O) system. *J. Eur. Ceram. Soc.*, 2000, **20**, 765–773.
11. Park, H. C., Lee, S. H., Ryu, B. K., Son, M. M., Lee, H. S. and Yasui, I., Nucleation and crystallization kinetics of CaO–Al_2O_3–$2SiO_2$ in powdered anorthite glass. *J. Mater. Sci.*, 1996, **31**, 4249–4253.
12. Yınnon, H. and Uhlmann, D. R., Applications of thermoanalytical techniques to the study of crystallization kinetics in glass forming liquids, Part I: theory. *J. Non-Cryst. Sol.*, 1983, **54**, 253–275.
13. Xu, X. J., Ray, C. S. and Day, D. E., Nucleation and crystallization of $Na_2O{\cdot}2CaO{\cdot}3SiO_2$ glass by DTA. *J. Am. Ceram. Soc.*, 1991, **74**(5), 909–914.
14. Li, W. and Mitchell, B. S., Nucleation and crystallization in calcium aluminate glasses. *J. Non-Cryst. Sol.*, 1999, **255**, 199–207.
15. Matusiata, K., Sakka, S. and Matsui, Y., Determination of the activation energy for crystal growth by DTA. *J. Mater. Sci.*, 1975, **10**, 961–966.
16. Donald, I. W., The crystallization kinetics of a glass based on the cordierite composition studied by DTA and DSC. *J. Mater. Sci.*, 1995, **30**, 904–915.
17. Romero, M., Rawlings, R. D. and Rincon, J. M., Development of a new glass-ceramics by means of controlled vitrification and crystallization of inorganic wastes from urban incineration. *J. Eur. Ceram. Soc.*, 1999, **19**, 2049–2058.
18. Sung, Y. M., The effect of additives on the crystallization and sintering of $2MgO$–$2Al_2O_3$–$5SiO_2$ glass–ceramics. *J. Mater. Sci.*, 1996, **31**, 5421–5427.
19. Matusita, K. and Sakka, S., Kinetic study on crystallization of glass by DTA-criterion on application of Kissinger plot. *J. Non-Cryst. Sol.*, 1980, **38-39**, 741–746.
20. Augis, J. A. and Bennet, J. E., Calculation of the Avrami parameters for the heterogenous solid state reactions using a modification of the Kissinger method. *J. Thermal. Anal.*, 1978, **13**(2), 283–292.
21. Ozawa, T., Kinetics of non-isothermal crystallization. *Polymer*, 1971, **12**, 150–158.
22. Kissinger, H. E., Reaction kinetics in differantial thermal analysis. *Anal. Chem.*, 1957, **29**, 1702.
23. Basal, N. P. and Doremus, R. H., *J. Thermal. Anal.*, 1984, **29**, 115.
24. Marseglia, E. M., *J. Non-Cryst. Sol.*, 1980, **41**, 31.
25. Erol, M., Genç, A., Öveçoğlu, M.L., Küçükbayrak, S., Taptık, Y. and Yücelen, E., Characterization investigations of a glass–ceramic produced from Çayırhan thermal power plant fly ashes. *J. Eur. Ceram. Soc.*, 2000, **20**, 2209–2214.
26. Matusita, K. and Sakka, S., *Bull. Inst., Chem. Res. Kyoto Univ.*, 1981, **59**, 159.
27. Davies, M. W., Kerrison, B., Gross, W. E., Robson, W. J. and Wichell, D. F., Slagceram: a glass-ceramic from blast-furnace slag. *Journal of Iron Steel Inst.*, 1970, **208**(4), 348–370.
28. Öveçoğlu, M. L., Microstructural characterization and physical properties of a slag-based glass-ceramic crystallized at 950 and 1100°C. *J. Eur. Ceram. Soc.*, 1998, **18**, 161–168.
29. Yılmaz, Ş., Özkan, O. T. and Günay, V., Crystallization kinetics of basalt glass. *Ceramics International*, 1996, **22**, 477–481.
30. Abel-Rahim, M. A., Ibrahim, M. M., Dongol, M. and Gaber, A., *J. Mater. Sci.*, 1992, **27**, 4685.
31. Kissinger, H. E., *J. Res. Nat. Bur. Standards*, 1956, **57**, 217.
32. Powder Diffraction File, Card No. 21-1276, 1992 Database Edition, Joint Committee on Powder Diffraction Standards (JCPDS), Swathmore, PA, USA.